Presented at ICMC2000, Rio de Janeiro, Brazil, June 11-15,2000

# Development of a $Nb_3Sn$ multifilamentary wire for accelerator magnet applications

M. Durante[a], P. Bredy[a], A. Devred[a], R. Otmani[b], M. Reytier[a], T. Schild[a], F. Trillaud[a]

[a]CEA/Saclay, DSM/DAPNIA/STCM, 91191 Gif-sur-Yvette CEDEX, France

[b]Alstom/MSA/Fil, 3Bis Avenue des trois Chênes, 90018 Belfort CEDEX, France

**Abstract –** CEA/Saclay and Alstom/MSA have carried out a program to develop a $Nb_3Sn$ multifilamentary wire for accelerator magnet applications relying on the internal-tin process. The main wire specifications are: an overall diameter of 0.825 mm, a critical current larger than 405 A at 4.2 K and 7 T, hysteresis losses lower than 450 mJ/cm$^3$ for a ± 3 T trapezoidal cycle, and a copper-to-non-copper ratio greater than 1. The last phase of the optimization program was based on four different strands and we present here the results of the characterization tests, including RRR, critical current and AC loss measurements.

**Keywords:** $Nb_3Sn$, internal-tin, AC losses, critical current

## I INTRODUCTION

CEA/Saclay has undertaken a R&D program to design and build a $Nb_3Sn$, single-aperture quadrupole magnet model relying on the same coil geometry as the LHC arc quadrupole magnets [1]. The nominal field gradient is 213 T/m at 4.2 K for a current of 12 000 A (without iron yoke). Such quadrupole magnet could be used for the final focus system of TESLA, the electron/positron linear collider now under study at DESY [2]. Wire design is inspired from ITER specifications [3], while cable design follows LHC outer cable specifications [4]. The program was started in 1996, in collaboration with Alstom/MSA/Fil, and has enabled Alstom to pursue its development of $Nb_3Sn$ wires and cables [5]. The wire optimization program described here has been carried out in parallel to a program investigating interstrand resistances in Rutherford-type cables [6] and a program evaluating different types of insulation systems for $Nb_3Sn$ magnets [7].

## II WIRE DESIGN

Alstom/MSA has developed four new layouts of $Nb_3Sn$ strands according to the internal-tin process. The four strands have a nominal diameter of 0.825 mm and a copper-to-non-copper ratio of about 1.4 to 1. They are made up of 19 multifilamentary bundles surrounded by a diffusion barrier and a copper outer sheath. Each bundle is composed of 198 Nb filaments, doped with 7.5wt. % Ta, arranged in four concentric circles around a Sn core. During the heat treatment required for $Nb_3Sn$ compound formation (660 °C for 240 hours, in a flow of Ar), tin diffuses through the copper matrix and reacts with the Nb filaments. The diffusion barrier prevents tin pollution of the copper outer sheath and preserves its resistivity. The bundles are twisted, with a pitch length of 10 mm. The main differences between the four strands are the bundle layout and the type of diffusion barriers. In two of the strands (referred to as B1 and B3) the multifilamentary bundles are spaced by six CuSn elements, while no CuSn spacers are introduced in the other two strands (referred to as B2 and B4). In addition, one strand of each type (B1 and B2) relies on a double Nb/Ta diffusion barrier, while the other two strands (B3 and B4) rely on a single Ta barrier. Removal of the Nb barrier is expected to reduce hysteresis losses. Salient strand parameters are summarized in Tab. 1, while cross-sectional views of strands B2 and B3 after heat treatment are presented in Fig. 1 and Fig. 2 respectively. The physical filament diameter is estimated to be of the order of 5 μm.

## III RESIDUAL RESISTIVITY RATIO

RRR (Residual Resistivity Ratio) measurements were carried out at Alstom/MSA on straight, 100-mm-long, samples of reacted strands. Resistivity is first measured at 273 K. The sample is then plunged into a liquid

helium bath and a small current is circulated in the sample while it is progressively removed from the bath. Low temperature residual resistivity is measured when the sample undergoes a resistive transition. Averaged RRR values over three samples per type of strands are presented in Tab. 2. All samples exhibit RRR values greater than 190. This indicates that the copper outer sheath has not been polluted during heat treatment and that the diffusion barriers did not break during wire processing. Examination of the cross-sectional views of the reacted strands (see Fig. 1 and Fig. 2) confirms the good quality of the diffusion barriers.

## IV CRITICAL CURRENT ON VIRGIN STRANDS

Critical current measurements on reacted strands were carried out at CEA/Saclay in a perpendicular magnetic field, at 4.2 K and at 1.8 K. The background field is provided by a hybrid NbTi/$Nb_3Sn$ superconducting solenoid capable of 12 T at 4.2 K, in a bore of 100 mm. The magnet and the sample holder have a common cryostat but two separate helium baths. A pumping system connected to an intermediate bath allows to cool down the sample bath to superfluid helium at 1.8 K and atmospheric pressure.

The $Nb_3Sn$ sample, about 1 m in length, is wound on the helicoïdal groove of a Ti cylinder, with a 32.5-mm diameter, according to VAMAS specifications [8]. Prior to winding, the Ti cylinder is coated with graphite powder to prevent sticking. Two copper rings are mounted at the top and bottom of the Ti cylinder and the strand ends are bolted to them to prevent motion during heat treatment. After reaction, the strand ends are soft-soldered to the copper rings, the screws are removed and the copper rings are gold-plated to provide a good contact surface for the current leads. The current is fed to the sample to produce outward Lorentz forces (self-field parallel to the applied field) in order to compensate for the thermal shrinkage differential between copper and $Nb_3Sn$. Two voltage tap pairs, spaced by 45 mm and 90 mm, are soldered to the sample, in the middle of the test section.

Measurements were carried out on three different samples per type of strands at 4.2 K and for magnetic flux densities in the range 5 to 12 T; one sample per type of strands was measured also at 1.8 K. The critical current, $I_C$, is estimated from the voltage-current curve using an electric field criterion of 0.1 μV/cm, while the resistive transition index, $n$, is determined in the range between 1 and 3 times the criterion. Fig. 3 presents a plot of the critical current density, $J_C$, over the non-copper cross-sectional area of the wire, vs. applied magnetic field, $B$, as measured on a B3 strand sample at 4.2 and 1.8 K (without self-field correction). The shift between the 4.2-K and the 1.8-K curves at high fields is of the order of 1.5 T. For all strands, the $J_C$ data are well fitted by a curve following Summers' parametrization [9]. Average values of measured critical current, $I_C$, and of resistive

transition index, $n$, at 4.2 K and 7 T are reported in Tab. 2, along with non-Cu critical current densities at 7 T and 12 T. The largest $J_C$ values are found for strands B1 and B3. These two strands, which also exhibit the largest $n$ values, satisfy the required $I_C$-criterion of 405 A at 7 T and 4.2 K.

## V AC-LOSSES

AC-loss measurements were performed at CEA/Cadarache on one sample per type of strand. The samples were wound on 20-mm-diameter, 91-mm-high TA6V cylinders and were heat-treated at CEA/Saclay. After reaction, they were transferred on G10 sample holders for magnetization measurements at CEA/Cadarache. The sample holder is mounted on an insert, shoved into the bore of a superconducting solenoid (capable of 5 T at 4.2 K, in a bore of 25 mm) and is cooled down to 4.2 K. Pick-up coils are placed on the sample holder to measure the applied field and the strand magnetization.

Magnetization cycles for ± 3 T and 1-3 T trapezoidal cycles were recorded for magnetic flux density sweep rates between 0.6 and 24 T/s. The losses at a given sweep rate are estimated by numerical computation of the area of the magnetization curve. The non-copper hysteresis losses, $W_h$, are determined by extrapolation of the losses vs. sweep rate curve at zero sweep rate, while the coupling-current time constant, $\tau$, is determined from the slope of the same curve (which is linear for all strands). As expected, for ± 3 T cycles, the strands with a double Nb/Ta barrier (B1 and B2) exhibit larger hysteresis losses than the strands with a single Ta barrier (B3 and B4). This can be explained by the additional losses generated at low fields in the niobium of the double barrier (Nb is a type-II superconductor with an upper critical magnetic flux density of 0.268 T at 4.2 K) [10]. An illustration of the Nb contribution can clearly be seen in Fig. 4, which compares the magnetization curves of strands B1 and B3. AC loss measurement results are summarized in Tab. 3. Effective filament diameter determination has been performed (according to Bean's model) using the hysteresis loss data for the 1-3 T trapezoidal cycles, where the Nb contribution is negligible.

## VI CONCLUSIONS

An optimization program, based on four 19-bundle wire layouts, has been carried out. Characterization tests, including RRR, critical current and AC-loss measurements, have been performed and results are satisfactory. Good values of RRR measured on reacted samples show that the diffusion barriers did not break during wire processing. The best combination of high $J_C$ and small effective filament diameter is obtained for the strand

referred to as B3, which has been selected for final production (five 60-m unit lengths of 36-strand Rutherford-type cable).

## ACKNOWLEDGEMENTS

The authors wish to thank G. Grünblatt (Alstom/MSA) and J.L. Duchateau (CEA/Cadarache) for their support of this program, C.E. Bruzek, for the definition of the strand layouts, and the dedicated teams at CEA/Saclay and CEA/Cadarache, which have helped setting up and carrying out the cryogenic tests.

## REFERENCES

[1] M. Peyrot et al., IEEE Trans. Appl. Supercond. Vol. 10 No. 1 (2000) pp. 170-173.

[2] $e^+e^-$ Linear Colliders : Physics and Detector Studies, DESY 97-123 (December 1997).

[3] P. Bruzzone et al., IEEE Trans. Magn. Vol. 30 No. 4 (1994) pp. 1986-1989.

[4] Internal Report LHC-MMS/97-153, CERN Geneva Switzerland (July 1997).

[5] C.E. Bruzek et al., Adv. Cryo. Eng. (Materials) Vol. 42B (1996) pp. 1369-1376.

[6] A. Devred et al., IEEE Trans. Appl. Supercond. Vol. 9 No. 2 (1999) pp. 722-726.

[7] A. Devred et al., Adv. Cryo. Eng. (Materials) Vol. 46 (2000) pp.143-150.

[8] L.F. Goodrich et al., Cryogenics Vol. 35 VAMAS Supplement (1995) pp. S19-S23.

[9] L.T. Summers et al., IEEE Trans. Magn. Vol. 44 No. 3 (1991) pp. 2041-2044.

[10] E. Gregory et al., IEEE Trans. Appl. Supercond. Vol. 7 No. 2 (1997) pp. 1498-1503.

**TABLES**

Tab. 1. Salient strand parameters.

| Strand Name | CuSn Spacers | Barrier | Cu/non-Cu |
|---|---|---|---|
| B1 | Yes | Nb/Ta | 1.37 |
| B2 | No | Nb/Ta | 1.34 |
| B3 | Yes | Ta | 1.41 |
| B4 | No | Ta | 1.41 |

Tab. 2. RRR and critical current measurements (on average over 2 or 3 samples).

| Strand Name | RRR | $I_C$ (1) (A) | $n$ (1) | non-Cu $J_C$ at 7 T (A/mm$^2$) | non-Cu $J_C$ at 12 T (A/mm$^2$) |
|---|---|---|---|---|---|
| B1 | 254 | 417 | 35 | 1850 | 765 |
| B2 | 228 | 404 | 21 | 1768 | 733 |
| B3 | 196 | 410 | 31 | 1846 | 751 |
| B4 | 225 | 390 | 26 | 1758 | 732 |

(1) At 4.2 K and 7 T.

Tab. 3. AC-loss measurements at 4.2 K.

| Strand Name | $W_h$ ± 3 T cycles (mJ/cm$^3$) | $\tau$ ± 3 T cycles (ms) | $W_h$ 1 – 3 T cycles (mJ/cm$^3$) | $\tau$ 1 – 3 T cycles (ms) | Effective Filament Diameter (μm) |
|---|---|---|---|---|---|
| B1 | 531.5 | 0.58 | 88.7 | 0.52 | 18.3 |
| B2 | 532.0 | 0.57 | 84.7 | 0.57 | 18.6 |
| B3 | 447.1 | 0.53 | 91.3 | 0.53 | 19.0 |
| B4 | 432.7 | 0.53 | 90.2 | 0.47 | 19.7 |

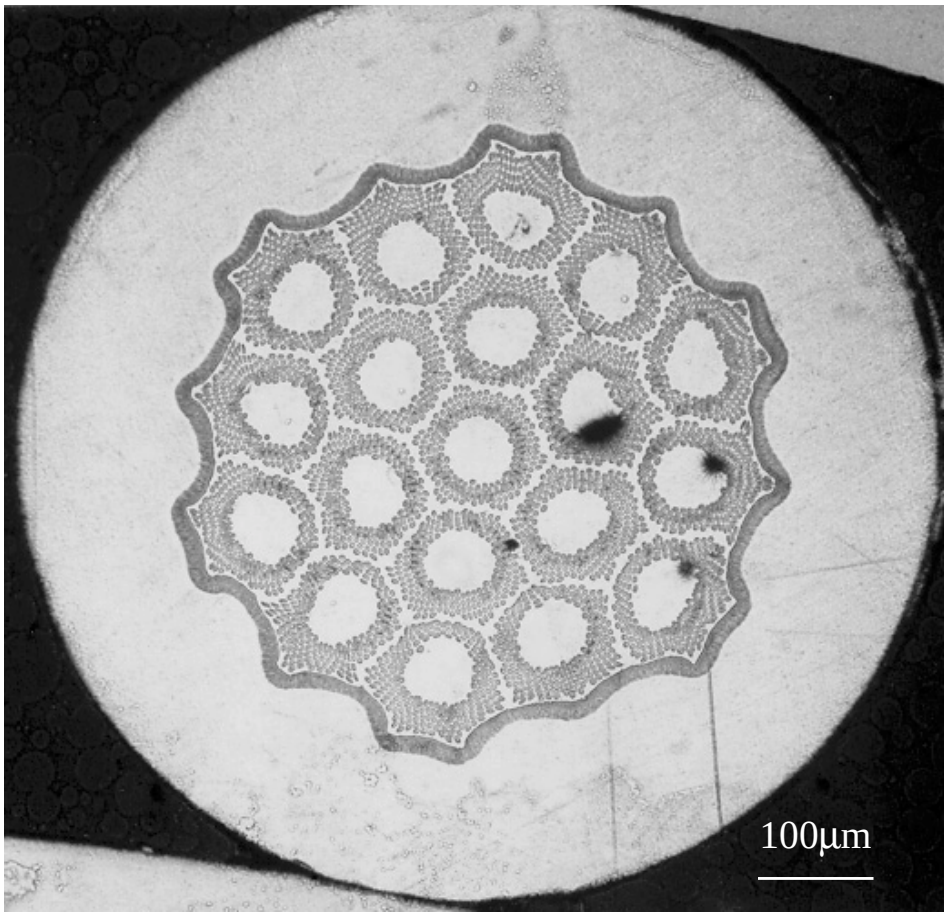


Fig. 1. Cross-sectional view of double-barrier strand B2 (no CuSn spacers), after heat treatment.

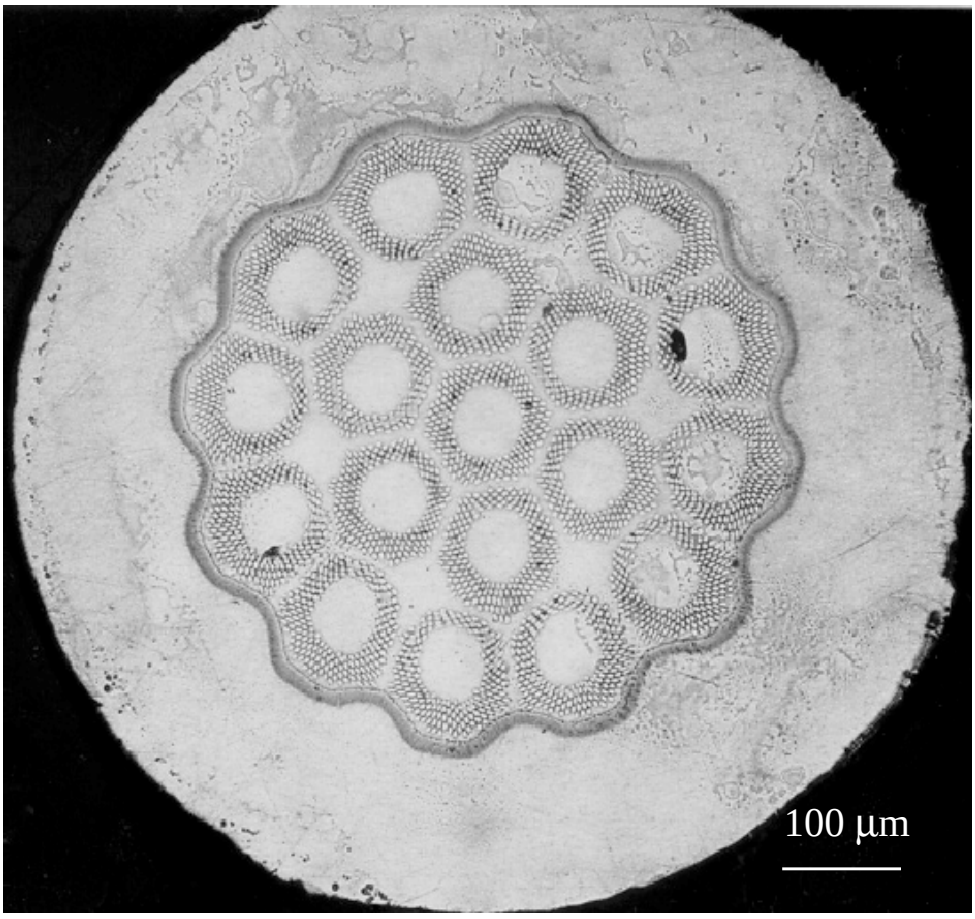


Fig. 2. Cross-sectional view of single-barrier strand B3 (CuSn spacers), after heat treatment.

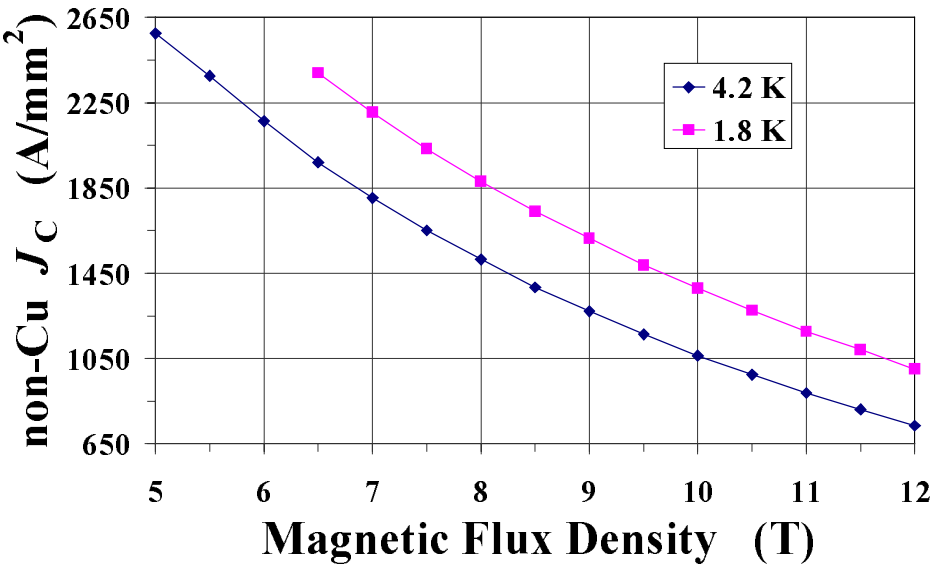


Fig. 3. Critical current density vs. magnetic flux density, as measured on a B3 strand sample, at 4.2 K and 1.8 K.

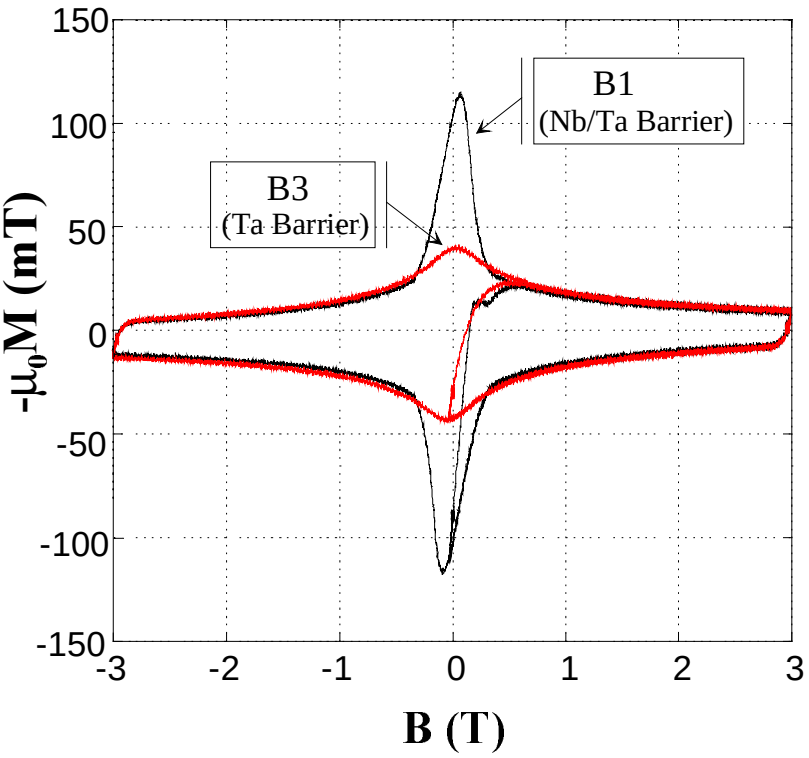


Fig. 4. Magnetization curves measured on strands B1 and B3,

for a ± 3 T trapezoidal cycle and a sweep rate of 1.5 T/s.